Proceedings of the 7th International Ship Stability Workshop, Shanghai, November 2004

THEORETICAL DEVELOPMENTS ON SURVIVAL TIME POST-DAMAGE

Andrzej Jasionowski*, **Dracos Vassalos**** **amd Luis Giarin***
* Safety At Sea Ltd, a.jasionowski@safety-at-sea.co.uk
** The Ship Stability Research Centre (SSRC), Universities of Glasgow and Strathclyde, d.vassalos@na-me.ac.uk

SUMMARY

This paper introduces a new reliability-based model for prediction of the rate of capsizing of a Ro-Ro vessel subject to SOLAS damage and random beam-on wave conditions. The concept has been verified successfully by means of comparison with available data from scaled-model experiments. Based on thus calculable probability to capsize, a model has been proposed to assess the distribution of the corresponding survival time of the vessel. A time-based criterion of survival has been proposed.

NOMENCLATURE

$\tilde{Q}_{in}$, $\tilde{Q}_{out}$	Rates of floodwater ingress and egress
t	Time variable
τ	Time integration variable
P_f	Probability of failure (capsize)
μ	Mean of the floodwater ingress or egress during one wave cycle
σ	Standard deviation of the floodwater ingress or egress during one wave cycle
μ_{out}	Mean of the total floodwater egress
σ_{out}	Standard deviation of the total floodwater egress
μ_{in}	Mean of the total floodwater ingress
σ_{in}	Standard deviation of the total floodwater ingress
n	Number of wave cycles
T_z	Zero crossing period
$f_{resistance}$	Probability density function of total floodwater egress
F_{demand}	Cumulative probability density function of total floodwater ingress
f_{KinQin}	Probability density function of floodwater ingress per wave cycle
f_{Kin}	Probability density function of ingress correction coefficient per wave cycle
f_{Qin}	Probability density function of ideal water ingress per wave cycle
f_R	Probability density function of relative motion at deck opening
m'_0	Variance of the relative motion
m_0	Variance of the wave motion
$S(\omega)$	Wave variance spectrum
a	Wave amplitude
f_{res}	Residual freeboard
l_{dam}	Damage width
f_{Kout}	Probability density function of egress correction coefficient per wave cycle
$f_{KoutQout}$	Probability density function of floodwater egress per wave cycle
K	Flooding correction coefficient
h_{SEM}	Head of added water on vehicle deck

1 INTRODUCTION

It has been recognized widely by the pertinent community that ship safety codes and regulations deriving from generalisations of often little-understood intricacies of damage stability, not only have failed to avert modern-world catastrophes of the MV Estonia dimension, but also impede the potential emergence of new generation optimal Ro-Ro ships, designed with inherently superior safety and enhanced commercial attractiveness.

One of the gaps still outstanding in providing for safety of Ro-Ro vessels is lack of guidelines in assessing rapidity of stability deterioration in case of hull breach and thus ensuring adequate time to orderly evacuate passengers and crew. Although new SOLAS Regulation 13-7.4, [11], in force since 1 July 1999, together with the IMO MSC/Circ.1033[1] set maximum evacuation time of passengers and crew at a level of no more than 60 minutes for newly built Ro-Ro vessels, no suitable technique has been proposed to date to efficiently demonstrate that the vessel can remain safe for this period of time in given conditions.

[1] Interim guidelines for evacuation analysis for new and existing passenger ships, June 2002

Although various studies on the aspect of ship survival time post-damage have been reported earlier, [2] - [7], none was able to conclusively recommend a methodology for its reliable assessments other than by way of tedious numerical simulations or model experiments.

This paper puts forward a simplified method to predict survival time of a ship subject to damage in beam-on waves.

There are three parts being addressed. Firstly, the hypotheses underlying the method are explained. Secondly, the method for predicting the probability to capsize, $\boldsymbol{P_f}$, is introduced briefly and discussed in detail in Appendix 1 and finally, a technique for rationalising survival time is presented.

2 APPROACH ADOPTED

The approach adopted in enumerating the phenomenon of ship survival time derives from closer analyses of the following observations:

(a) Damage Ro-Ro ship capsize is governed by the process of floodwater accumulation.
(b) Statistics of the two phenomena governing this process (floodwater ingress and egress) can be described independently of each other.
(c) A ship's instantaneous heeling in damaged condition can be regarded as an oscillatory response of very low frequency and as such it can be considered as a stationary process.

The first observation, that a ship capsize is governed by the floodwater accumulation is widely recognised and needs no further elaboration here. However, the two other observations need justification as discussed in the following.

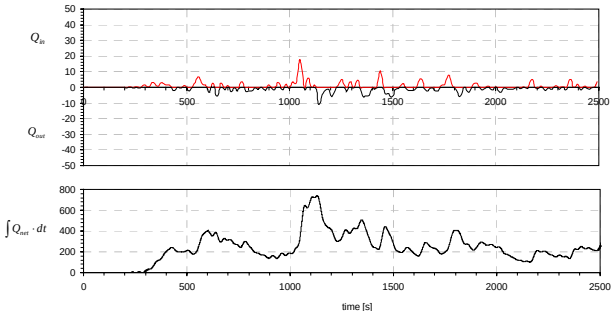

Figure 1 Time series of ingress and egress rates, Q_{in} and Q_{out}, respectively, averaged over a wave cycle (upper plot) and floodwater accumulation, $\int Q_{net} \cdot dt$, (lower plot), Run 101 (ref [4]).

2.1 Statistical independence of floodwater ingress and egress

It must be stated clearly here, that the division between the processes of floodwater ingress and egress is a hypothesis. It greatly simplifies the mathematical construct describing the survivability of a Ro-Ro vessel, and its justification derives from the following arguments.

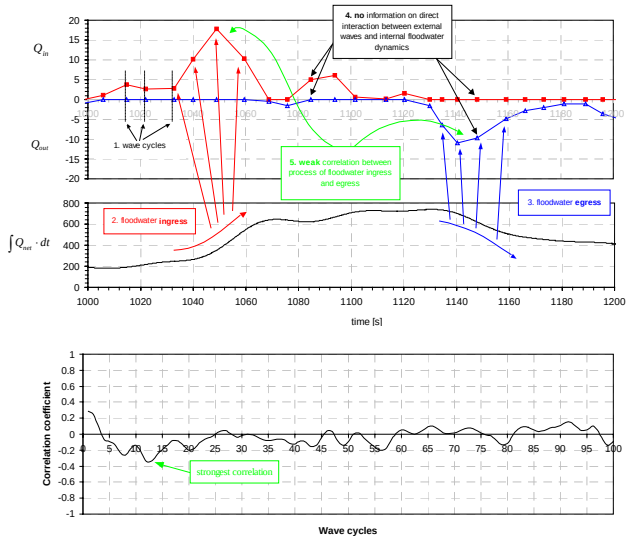

Figure 2 Close-up of time series of Figure 1, (upper and mid graph), and coefficient of correlation between ingress and egress rates (lower graph). Averaging of the net inflow/outflow following each wave pass is discussed also in Appendix 1.

Firstly, any interaction between ingress and egress is simply not quantifiable with the available data (gradients of instantaneous floodwater accumulation, as is highlighted by points "2" and "3" in Figure 2). Although ingress and egress rates vary with time, either of the processes overrides the other at any instant of wave passage, (i.e. on average the water either flows in or out and no knowledge can be inferred on the cause of the variability of the flow, see point "4" in Figure 2). To quantify the level of interactions between water flowing in and out, far more sophisticated techniques, e.g. involving laser, for measurements of velocities of fluid particles preferably over three-dimensional space in the vicinity of the damage opening would be required. However, it is argued in this work that such in-depth experimentation, not to mention any mathematics relevant to ensuing analyses and modelling, would defy the purpose of this work, namely to derive a method, which can model the main mechanisms governing ship survivability in a simplified and usable manner.

Secondly, the correlation between water ingress and egress is found to be weak, with Pearson's linear correlation coefficient of 0.285, see the lowest diagram

of Figure 2. In other words, average water ingress within a wave cycle will not result in equivalent average water egress over the next cycle. It will take a number of 10-15 wave cycles, within which water ingress accumulates, to notice fairly equivalent water discharge, though quite a number of wave cycles afterwards, see point "5" in Figure 2. Therefore, it is assumed here that this correlation is negligible and that the statistics describing ingress or egress can be derived independently of one another.

The above assumptions give rise to the core hypothesis of this research, namely that the capsizing of ships with large undivided spaces, subject to side damage and exposed to wave action can be considered through modelling in terms of a reliability problem. The *external demand* (load in case of structural analyses) is signified by the floodwater ingress, and the *internal resistance* (limiting strength in structures) is signified by floodwater egress. The interaction of load (water ingress) and resistance (water egress) results in a time-varying state of the vessel. The state of the vessel, in turn, is a function of the amount of floodwater accumulated on the vehicle deck. It follows from this reasoning that capsizing events can be characterised in terms of a *probability of limit state violation (probability of failure)* $\boldsymbol{P_f}$, representing likelihood that cumulative water ingress exceeds cumulative water egress, $\int_t \tilde{Q}_{in} > \int_t \tilde{Q}_{out}$.

Note here that in the proposed method, it is irrelevant by how much the accumulated ingress exceeds the accumulated egress, which would need to be considered in the physical estimation of a critical amount of net inflow leading to vessel capsize. As shown in Appendix 1, the expression on the egress process caters for the critical amount of floodwater present on the ship inherently and, therefore, comparing $\int_t \tilde{Q}_{in}$ and $\int_t \tilde{Q}_{out}$ would provide a direct measure of probability of failure.

2.2 Heeling as a stationary process

The final assumption introduced in the development of the method for time-based assessment of ship survivability, relates to interpretation of the probability of failure $\boldsymbol{P_f}$. Namely, it is considered independent of time for a given set of ship and environmental parameters, and as such it can be interpreted as a constant parameter of the most basic random process, the Bernoulli trial process .

Thus, the $\boldsymbol{P_f}$ (or method of its estimation) implies that the underlying statistics of floodwater ingress and egress do not change in time for a set of ship and environmental parameters. This assumption derives, in turn, from an observation that for given set of ship and sea conditions, whereby the floodwater egress matches or exceeds the ingress, the heel response resembles an oscillatory process with constant statistics (mean, stdev, etc), in particular when viewed in the context of infinite time, see Figure 3. Hence, the quasi-stationary character of heel can justify the above assumption of independence of $\boldsymbol{P_f}$ on time exposure to the sea environment[2]. In other words, if the probability to capsize is $\boldsymbol{P_f}$ =0, then it remains so regardless whether it is evaluated for 30 minutes or 180 minutes.

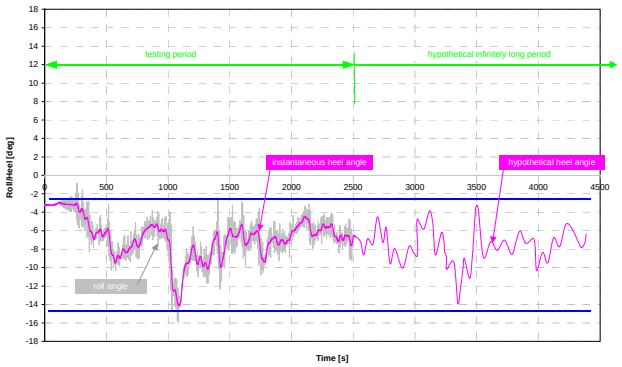

Figure 3 Roll and heel angle of damaged ship subject to wave action. The heel angle can be considered as a quasi-stationary process when the floodwater egress matches or exceeds the wave capability to accumulate water on the vehicle deck.

Before embarking on further details of the proposed concept, it must be emphasised here that any of the separate hypotheses described above are an integral part of the method for survivability assessment. While these assumptions can be disputed to a greater or lesser extent when viewed on their own, the ultimate measure of the merit of these hypotheses shall derive from comparisons of survival predictions with the reference experimental data.

The aforementioned model together with comparative studies between theoretical and experimental results form the remaining part of this paper.

3 SURVIVABILITY PREDICTION BASED ON RELIABILITY THEORY

Since their introduction in the 50's by Pugsley and Freudenthal, [14], reliability methods have seen drastic increase in their use in many industrial sectors. The advantages of these approaches are that over design can be avoided, uncertainties can be handled in a logical way, sensitivity to variables assessed and a more rational basis for decision making followed. The methods have been extensively applied in the nuclear, offshore, rail, shipping,

[2] Provided the exposure considered allows meaningful representation of the sea state, hence 30 minutes is the required minimum

aerospace, bridge, building, process plant and pipeline industries. Failure processes that can be addressed include fracture, collapse, fatigue, creep, corrosion, bursting, buckling, third party damage, stress corrosion and seismic damage.

The fundamental concept of reliability analysis is that resistance and demand factors are statistical quantities with a central tendency (mean), dispersion about the mean (variance) and some form of distribution (probability density function, e.g. Normal). When combined together via a suitable expression to describe the limit state (such as fracture, collapse or capsize in this case) there will be a finite probability that the demand will exceed the resistance. This defines the probability of failure, $\boldsymbol{P_f}$, and since reliability is equal to 1-$\boldsymbol{P_f}$, the inherent reliability of a system with given resistance properties against a particular failure mode is defined.

The expression for limit state violation, i.e. evaluation of $\boldsymbol{P_f}$, can be derived as convolution of the corresponding probability density functions of demand and resistance, given that the statistical distributions of these two variables are independent. This is the most common approach applied today in structural engineering, and is referred to as the 2nd moment First Order Reliability Methods (FORM). As introduced in the §2, this is the proposed technique for evaluation of capsizal probability of a vessel with set parameters in a given sea state. The final formula is presented here as (1) with graphical illustration in Figure 4.

$$P_f = \int_{-\infty}^{\infty} f_{resistance}(\tau, \mu_{out}, \sigma_{out}) \cdot (1 - F_{demand}(\tau, \mu_{in}, \sigma_{in})) \cdot d\tau \qquad (1)$$

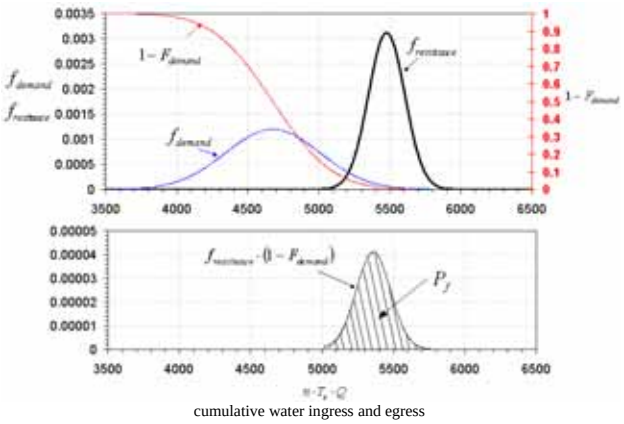

Figure 4 Concept of probability of limit state violation based on reliability theory, see Appendix 1

Naturally, the core of the method revolves around the form of the integrand functions and the basis of the integration. The details of these functions with relevant verification studies demonstrating ability of (1) to predict survivability of damaged passenger Ro-Ro vessels is given in Appendix 1.

To summarise the development shown in Appendix 1, the following table lists all ship- and environment-related input parameters pertinent to (1):

f_{res}	residual freeboard
h_{SEM}	floodwater head pressure
l_{dam}	damage longitudinal extent
H_s	significant wave height
T_z	zero crossing period

The computed from (1) output is the probability to capsize, $\boldsymbol{P_f}$, for given ship conditions operating in A specific sea state, see right diagram of Figure 5. A fairly common way of presenting these predictions is shown in the left side of Figure 5. Based on estimates of probability to capsize for a whole range of sea states and a number of KG values (with the rest of ship conditions fixed) a survival "band" introduced in other phases of this project, [2], can be derived.

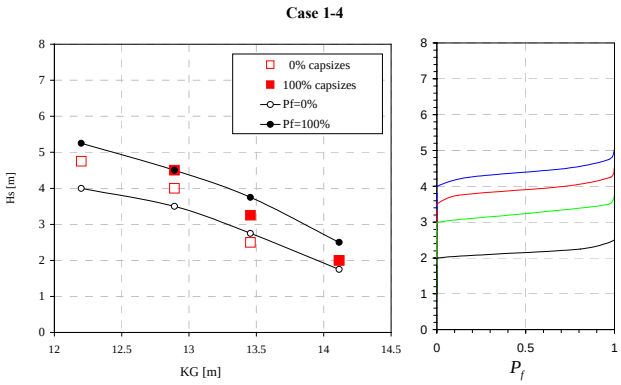

Figure 5 Survival boundaries for cases 1-4 from ref [4] (left plot) - comparison between experiment (red squares) and the reliability-based technique (black/white circles with black line)and distribution of probability to capsize for four KG values (right plot)

The next chapter demonstrates how predicted probabilities to capsize, $\boldsymbol{P_f}$, form the basis for estimations survival time.

4 SURVIVAL TIME ASSESSMENT

As discussed in the foregoing, capsizing of a ship in an environment can be characterised by the parameter $\boldsymbol{P_f}$. Given the assumptions that the probability of capsize $\boldsymbol{P_f}$ is constant for given set of ship and sea state parameters, capsizing can be considered in terms of a Bernoulli trial

process[3]. For such process with constant parameter ***P***, the statistical density function ***c*** of the number ***n*** of experiments to obtain a first desired outcome is given by the geometric probability density function:

$$c = n \cdot P \cdot (1-P)^{n-1} \qquad (2)$$

The cumulative geometric probability distribution function is given as:

$$C = 1-(1-P)^{n} \qquad (3)$$

Formulae (3) defines the probability (confidence level) that the $\boldsymbol{n}^{th}$ test is a "success" given constant probability *P* of "success" in each test ("success" is taken as vessel capsize). Also a test in this work pertains to an experiment lasting 30 minutes within which capsize is to be observed with constant rate of $\boldsymbol{P_f}$. Hence, the cumulative time t_{cap} (in minutes) within which capsize is to occur with confidence level of C_{cap} can be found as $t_{cap} = n \cdot 30$. This time is basically the minimum survival time of the vessel subject to damage and wave excitation. For instance, a statement that the time to capsize is 40 minutes with confidence of no more than 5% is equivalent to stating that:

- The likelihood that capsize will happen after 40th minute is 95% or that
- The time of survival is 40 minutes with confidence of 95%.

Deriving from the above, the relationship between survival time $\boldsymbol{t_{cap}}$, constant rate of capsizing in given environment $\boldsymbol{P_f}$ and the confidence level of certain capsize occurrence $\boldsymbol{C_{cap}}$ within a series of $\boldsymbol{n=t_{cap}/30}$ tests can be written as follows:

$$C_{cap} = 1-(1-P_f)^{\frac{t_{cap}}{30}} \qquad (4)$$

By assuming fixed confidence level of capsize occurrence, the following expression of survival time can be derived from (4):

$$t_{cap} = 30 \cdot \frac{\ln(1-C_{cap})}{\ln(1-P_f)} \quad \text{[minutes]} \qquad (5)$$

Given estimates of the $\boldsymbol{P_f}$ for a range of ship and environmental parameters, the survival time boundary curves for any arbitrary confidence level can be derived as shown in Figure 6 (or Figure 7).

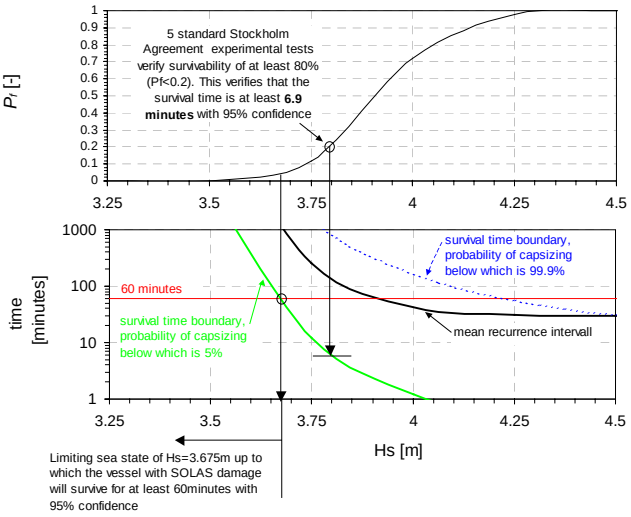

Figure 6 Explanation of time based survivability assessment, sample vessel conditions

As it can be seen on this sample, assuming a confidence level of 95% that the damaged vessel survives above given time and that the minimum time the vessel is to survive is 60 minutes, allows for estimates of the limiting environmental conditions for this vessel in terms of significant wave height, namely $H_s \le 3.675m$.

Following this reasoning, it is possible to derive time-based survival boundaries for any required confidence level, thus establishing a relationship between ship operational and environmental conditions. To do so it is convenient to derive from (4) an expression for $\boldsymbol{P_f}$ which can then be used to find limiting curves between the ship and the environmental conditions through (1).

$$P_f = 1-e^{\ln(1-C_{cap})\frac{30}{t_{cap}}} \qquad (6)$$

Thus by comparing (1) and (6) with fixed C_{cap} and/or t_{cap} time-based boundary curves can be derived as shown in Figure 7.

Of note in Figure 7 is the exponential trend of the survival time at the lower part of the survivability boundary, which trend was originally pointed out in phase 1 of this project (1996/1997), [3]. As the critical sea state approaches levels where the vessel does not capsize, the survival time increases very rapidly, theoretically to infinity.

[3] A sequence of independent experiments each of which has the same probability of success ***P***, such as for instance coin tossing, where probability of obtaining tail is constant ***P***=0.5

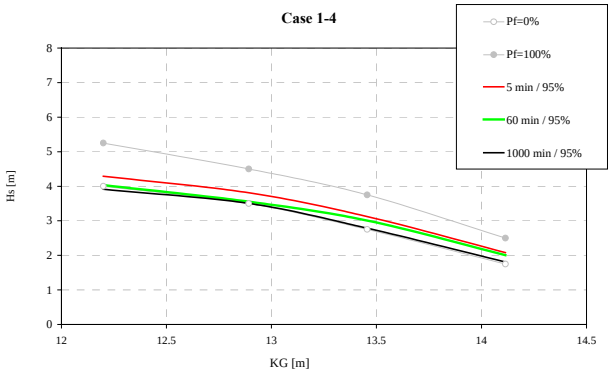

Figure 7 Survival time-based boundary curves

One of the nuances deriving from Figure 6 and Figure 7 is how to practically (experimentally) verify the survival time and hence, what level of survival time should be required.

For instance, applying concepts proposed in this paper to explain the underlying trends in Stockholm testing, it can be seen in Figure 6, that the standard 5 Stockholm survivability tests of 30 minutes duration could only verify survival time of only 6.9 minutes (with 95% confidence), and that to verify time of 60 minutes, approximately n=40 tests would be required (***n≥ 1 / P$_f$***, where ***P$_f$=0.025*** from (6) for ***C$_{cap}$=0.05*** and ***t$_{cap}$=60*** minutes, note that (***1 / P$_f$***) is the well know definition of the mean recurrence interval).

Clearly, such level of survival time is not practical for experimental verification.

However, as can be seen in Figure 6, the difference in significant sea state where the survival time rises from 6.9 (***P$_f$***=0.2) to 60 (***P$_f$***=0.025) minutes is of the order of the resolution used to experimentally establish the boundary, i.e. less than Δ Hs=0.25m. It is proposed to use this characteristic as well as knowledge of the trends on survival time, (5) and (6) with (1), to propose a time-based survival criterion.

4.1 The Proposed Time-Based Survival Criterion

Suppose that the time of 60 minutes is set as the minimum required for a vessel to sustain its stability when subjected to the worst SOLAS damage. Since survival time is a random variable, it is also required that this level of time is assured with confidence of 95%. Given that the time of vessel foundering is governed by a scenario involving large scale flooding of undivided spaces (e.g. not by sinking), to ensure this survivability the vessel (KG, loading, freeboard, etc) and the environment (H_{crit}) operational conditions must be such that[4]:

$$P_f \le 0.025 \qquad (7)$$

Where P_f is given by (1).

Experimental verification would entail a number of ***n*** tests lasting at least 30 minutes each at a sea state corresponding[5] to $P_f = \frac{1}{n}$.

5 CONCLUSIONS

This paper introduced a new approach for predicting ship survival by means of a reliability-based concept of estimating probability of failure (capsize). The concept has been verified by means of comparison with extensive database of model experiments derived in an earlier phases of this project. Very good agreement has been demonstrated.

Based on thus calculable probability to capsize, a model has been proposed to assess the distribution of the corresponding survival time of a damaged Ro-Ro vessel. A tentative survival-time-based criterion has been proposed.

Although vessel capsize is a case of limit state behaviour, a physical process that is highly sensitive to variation of many governing factors, it is anticipated that the newly derived method will become the ultimate functional representation of this sensitivity, well suited for engineering application.

6 ACKNOWLEDGEMENTS

This research has been funded partly by the MCA Project RP498 and partly by the Marie Curie Industry Host Fellowship, Contract No MCFH/ 2000/00240-SI2.327090/SaS. The experimental data have been derived during Phase II of the research into the time-based survival criteria for Ro-Ro vessels funded by the UK MCA, with partial support of the European Commission DG Research project HARDER, Contract No GRD1-1999-10721. All this support is gratefully acknowledged.

[4] The criterion (7) can be set for arbitrary level of survival time and/or confidence level by use of formulae (6)

[5] For example, considering a vessel with given set of conditions as used in Figure 6, to verify 60 minutes (95% confidence) survivability for operation at limiting sea state of ***H$_{crit}$*** = 3.675m, five tests with no capsizing event would be required at *Hs*~3.8m (*P$_f$*=0.2), or two tests at *Hs* ~3.9m (*P$_f$*=0.5), etc, as derived from the relation between the ***Hs*** and ***P$_f$***.

REFERENCES

[1] **Vassalos, D., Pawłowski, M., and Turan, O**., *"A theoretical investigation on the capsizal resistance of passenger Ro/Ro vessels and proposal of survival criteria"*, Final Report, Task 5, The North West European R&D Project, March 1996.

[2] **Dracos Vassalos, Andrzej Jasionowski, Kieran Dodworth**, *"Assessment of Survival Time of Damaged Ro-Ro Passenger Vessels"*, Final Report to MCA, 02-98-1AJ-1IS, February 1998

[3] **Jasionowski, A, Dodworth, K and Vassalos, D**: *"Proposal of Passenger Survival-Based Criteria for Ro-Ro Vessels"*, International Shipbuilding Progress, Vol. 46, No 448, October 1999.

[4] **Vassalos, D, Jasionowski, A, Shu Hong Chai, Samalekos, P**, *"Time-based survival criteria for Ro-Ro vessels, Phase II"*, Draft Final Report for UK MCA, January 2001.

[5] **Jasionowski, A, Vassalos, D, Guarin, L**, *"Time-based Survival Criteria for Passenger Ro-Ro Vessels"*, Proceedings of the 6th International Ship Stability Workshop, Webb Institute, New York, October 2002

[6] **Kat de, Jan, Veer Riaan van't**, "Mechanisms And Physics Leading To The Capsize Of Damaged Ships", 5th International Workshop, University of Trieste, 12-13 September 2001.

[7] **Jasionowski, A, Vassalos, D,** *"Research Project RP498 Time-Based Survival Criteria For Passenger Ro-Ro Vessels, Phase III"*, Final Report For The UK Maritime And Coast Guard Agency, March 2004.

[8] **Wood, Allan, G**, *"Validating Ferry Evacuation Standards", RINA INTERNATIONAL CONFERENCE in association with The Nautical Institute on: "Escape, Evacuation & Rescue Design for the Future"*, 19&20 Nov. 1996, London

[9] **Guro Christiansen**, *"A Report on the State of the Art of Evacuation and Crowd Simulation"*, The Ship Stability Research Centre, SSRC-05-00-GC-01-IR, May 2000

[10] **Pawlowski**, M, *"Accumulation of water on the vehicle deck"*, Proceedings of the Institution of Mechanical Engineers, Part M: Journal of Engineering for the Maritime Environment, 2003, Vol. 217 (M4), pp. 201-211.

[11] SOLAS, 2002

[12] **Robert E Melchers**, *"Structural reliability analysis and prediction"*, John Wiley & Sons, Second Edition, The University of Newcastle, Australia, 1999

[13] **Shiff Daniel, D'Agostino Ralph B**, *"Practical Engineering Statistics"*, John Wiley & Sons, 1996

[14] **Corus UK Limited**, "Methods, Applications and Software for Structural Reliability Assessment", Swinden Technology Centre, Moorgate, Rotherham S60 3AR, Fax: (01709) 825337, Telephone: (01709) 820166, 21 August 2001

APPENDIX 1 PRDICTIONS OF SURVIVABILITY BASED ON RELIABILITY CONCEPT

1 Introduction

As has been discussed in the main body of this paper, a reliability-based model of ship survivability has been proposed, as given by equation (1).

This Appendix explains forms of the integrand functions of the above model and demonstrates capabilities of this solution by comparison with available model scale experiments.

The integrand functions of (1) are the density functions of the water that can be accumulated or discharged from the Ro-Ro vehicle deck within given testing period of time. These functions have been identified as normal distributions deriving from the statistical law of central limit theorem. The central limit theory states fundamentally that distribution of an average will tend to be normally distributed regardless of the distribution from which the average derives. Thus, given any statistical distribution of random variable, say, water ingress rates, $\tilde{Q}_{in}$ with corresponding mean μ and standard deviation σ, the expected distribution of the sum of **n** ingress rates, $\sum \tilde{Q}_{in}$, will be normally distributed with mean $\mu_{in} = n \cdot \mu$ and standard deviation $\sigma_{in} = \sqrt{n} \cdot \sigma$.

This is the theory underlying the component functions of formulae (1), as discussed next.

2 Demand function – floodwater ingress

The central limit theory, allows constructing of the demand function as the cumulative normal distribution function, which is given as (8):

$$F_{demand}\left(x, \mu_{in}, \sigma_{in}\right) = \frac{1}{\sqrt{2 \cdot \pi}} \int_{-\infty}^{x} \frac{1}{\sigma_{in}} \cdot e^{-\frac{(\tau - \mu_{in})^2}{2 \cdot \sigma_{in}^2}} \cdot d\tau \qquad (8)$$

Where:

$$\mu_{in} = n \cdot T_z \cdot \int_0^\infty Q \cdot f_{K_{in}Q_{in}}(Q) \cdot dQ \qquad (9)$$

Is the mean of the total floodwater ingress taking place within time of $n \cdot T_z$ seconds, and

$$\sigma_{in} = \sqrt{n \cdot T_z^{\,2} \cdot \int_0^\infty (Q - \mu_{in})^2 \cdot f_{K_{in}Q_{in}}(Q) \cdot dQ} \qquad (10)$$

Is the standard deviation of the total floodwater ingress taking place within time of $n \cdot T_z$ seconds.

The formulations (9) and (10) derive from a probability density function of floodwater ingress rates, $f_{K_{in}Q_{in}}(Q)$, per one cycle of wave elevation relative to the deck edge at the opening with assumed constant zero crossing period. The randomness of ingress rates derives from (a) the randomness of the sea waves exacerbated by the vessel response, (b) the non-stationary character of the interaction between the outside wave field and the dynamically responding water sloshing on the vehicle deck, both strongly affected by the vessel motion, and (c) from the discontinuous character of the flow through openings located some distance above the waves.

It has been proposed in this project to construct this function as a convolution of the theoretical distribution $f_{Q_{in}}(Q)$ of the values of inflow flooding rates derived from Bernoulli equation, with an assumption that no water is present on the vehicle deck, and the distribution of a correction coefficient $f_{K_{in}}(K)$, whose purpose is accounting for all the remaining effects mentioned above and derived through regressions on experimental data. Given formulation of both of these functions, the probability density function of the water ingress can be found from the following integral (11):

$$f_{K_{in}Q_{in}}(Q) = \int_0^\infty \frac{1}{|\tau|} \cdot f_{Q_{in}}(\tau) \cdot f_{K_{in}}\left(\frac{Q}{\tau}\right) \cdot d\tau \qquad (11)$$

Note that function (11) signifies an assumption of statistical independence between the density functions of K and Q. This has so far been justified *ad hoc* by good agreement with the actual ingress rates measured experimentally, see Figure 8 below.

Note that the coefficients K_{in} are derived from empirical data, whereby the theoretical ingress has been assumed and the relative ratio between the actual flow and the theoretical one used to find the K_{in}, see (24) and Figure 12.

The question now arises as to the details of the integrand functions of formulae (11), i.e. probability density functions $f_{K_{in}}$ and $f_{Q_{in}}$.

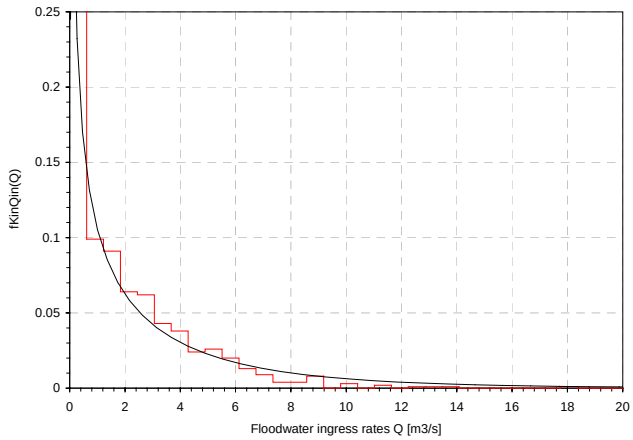

Figure 8 Sample probability density function of inflow rates, comparison with experiment (Case 2, Hs=4.0m)

The theoretical density distribution of ingress flooding rates is derived by substitution of the variable in the Rayleigh probability density function of wave excursions, corrected for the slight increase in the spectral energy of relative motion. The substituted variable is that of ingress flooding rate corresponding to relative wave amplitude and evaluated for the average wave cycle duration characterised by zero crossing period, see (18) and Figure 10. The corresponding function will be of the following form (12):

$$f_{Q_{in}}(Q) = f_R(a(Q)) \cdot \left|\frac{da(Q)}{dQ}\right| \qquad (12)$$

Where:

$$f_R(a) = \frac{a}{m'_0} \cdot e^{-\frac{a^2}{2 \cdot m'_0}}$$ Rayleigh probability density function of relative motion at the deck edge. (13)

$$m'_0 = 4^{2 \cdot p - 2} \cdot m_0^p$$ Variance of the relative motions (14)

p=1.17 Power in the relationship between the wave motion and relative motion (15)

$$m_0 = \int_0^\infty S(\omega) \cdot d\omega$$ Variance of the wave motion (16)

$S(\omega)$ Wave variance spectrum (17)

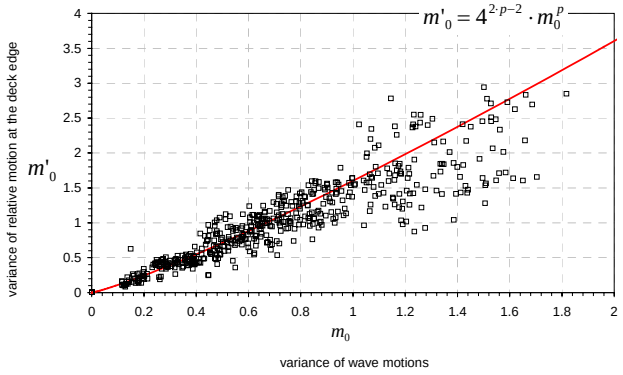

Figure 9 A relationship between the wave motion and relative motion as measured during experiments on PRR1 vessel

It must be stressed here, that the coefficient (15) proves to be highly influential on the ultimate outcome of survivability from (1), therefore its present value has been derived from matching of the survival boundaries rather than regression on relative motion. One of the reasons for this is the fact that the experimental data shown in Figure 9 are contaminated by inaccuracies due to ship radiation wave field as well as reflections from both the ship and the walls of the experimental tank. Nonetheless, as can be seen in Figure 9, the present result can still be regarded as representative of the phenomenon of relative motion.

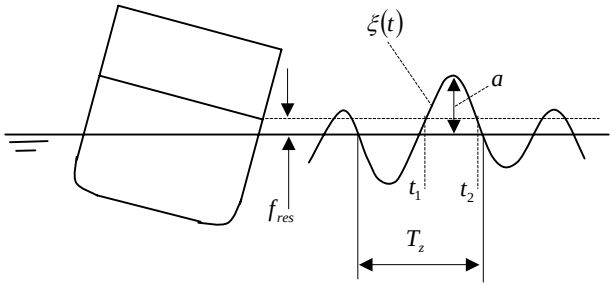

Figure 10 Simplified modelling of water ingress on a Ro-Ro car deck

In addressing the process of floodwater ingress caused by the action of waves, a simplified modelling was adopted in this research. More specifically, the following idealistic model was adopted:

$$Q_{in} = \int_{t_1}^{t_2} \sqrt{2\cdot g\cdot h}\cdot dA\cdot dt\cdot\frac{1}{T_z} \qquad m^3/s/cycle \qquad (18)$$

Where:

$$t_1 = \frac{T_z}{2\cdot\pi}\cdot\sin^{-1}\left(\frac{f_{res}}{a}\right) \qquad f_{res}\le a \qquad (19)$$

$$t_2 = \frac{T_z}{2} - t_1 \qquad (20)$$

$$h = \xi(t) - f_{res} \qquad (21)$$

$$\xi(t) = a\cdot\sin\left(\frac{2\cdot\pi}{T_z}\cdot t\right)$$ Relative motion at the opening edge (22)

$$dA = h\cdot l_{dam} \qquad (23)$$

f_{res} Residual freeboard

l_{dam} Damage width

The relationship between the ingress rates and wave amplitude in (18) is rather complex, therefore at present the inverse function $a(Q)$ of (18) and applied in (12) is found by linear interpolation, see Figure 11 below.

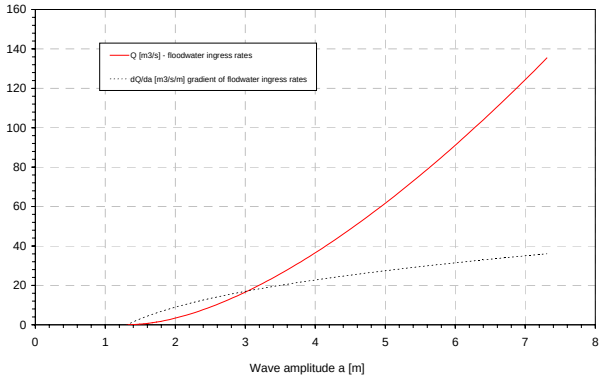

Figure 11 Sample floodwater ingress functions derived from (18), freeboard 1.308m

As mentioned above, the integrand function $f_{K_{in}}$ is found through regression on empirical data. The following log-normal probability density function with its coefficients was found to fit the data, see Figure 12.

$$f_{K_{in}}(K) = \frac{1}{\sqrt{2\cdot\pi}\cdot\sigma_{K_{in}}\cdot K}\cdot e^{-\frac{1}{2\cdot\sigma_{Kin}^2}\cdot(\ln(K)-\mu_{Kin})^2} \qquad (24)$$

$$\mu_{K_{in}} = -0.612$$

$$\sigma_{K_{in}} = 0.321$$

Constant regression coefficients (25)

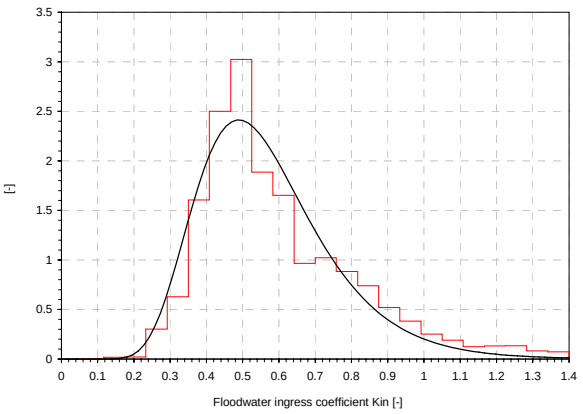

Figure 12 Fitted probability density function of ingress coefficient, comparison with experimental data

The spread in the flooding coefficient shown in Figure 12 must be viewed with some care. Namely, it cannot be directly regarded as the flow coefficient of typical fluid flow through weir openings, as the coefficient derived in this study corresponds to flow energy loss averaged over wave cycle, or indeed, to flow energy gain, since it exceeds the value of 1.0. Note that the energy gain is likely a result of added momentum to the flow by the relative motion between the ship and the incident wave field, not present in assumptions of the equation of steady flow of ideal fluid, (18).

3 Resistance function – floodwater egress

The second integrand function of equation (1) deriving from central limit theorem is that of probability density function of cumulative floodwater egress, representing vessel's ability to withstand the effects of wave action by continuous discharge of the floodwater from the vehicle deck. The function is that of normal distribution given by equation (26).

$$f_{resis\tan ce}(x,\mu_{out},\sigma_{out}) = \frac{1}{\sqrt{2\cdot\pi}\cdot\sigma_{out}}\cdot e^{\frac{1}{2\cdot\sigma_{out}^{\,2}}(x-\mu_{out})^2} \qquad (26)$$

Where:

$$\mu_{out} = n\cdot T_z\cdot\int_0^{\infty} Q\cdot f_{K_{out}Q_{out}}(Q)\cdot dQ \qquad (27)$$

Is the mean of the total floodwater egress taking place within time of $n\cdot T_z$ seconds, and

$$\sigma_{out} = \sqrt{n\cdot T_z^{\,2}\cdot\int_0^{\infty}(Q-\mu_{out})^2\cdot f_{K_{out}Q_{out}}(Q)\cdot dQ} \qquad (28)$$

Is the standard deviation of the total floodwater egress taking place within time of $n\cdot T_z$ seconds.

In a manner similar to the demand function, the expected value and standard deviation of the floodwater egress, equations (27) and (28) respectively, derive from a probability density function of floodwater egress rates, $f_{K_{out}Q_{out}}(Q)$, per one wave motion cycle. In this case, however, the randomness of egress rates is assumed to derive mainly from the non-stationary character of the interaction between the outside wave field and the dynamically responding water sloshing on the vehicle deck, again, strongly affected by the vessel motion. The result of this assumption is that the theoretical flooding is always constant for given head of water on the vehicle deck, and the randomness present is modelled by deriving the density function of correction coefficient, $f_{K_{out}}$. Thus, for given function $f_{K_{out}}$ the $f_{K_{out}Q_{out}}$ can be estimated by variable substitution as follows:

$$f_{K_{out}Q_{out}}(Q) = f_{K_{out}}(K_{out}(Q))\cdot\frac{1}{Q_{out}} \qquad (29)$$

Where:

$$K_{out}(Q) = \frac{Q}{Q_{out}} \qquad (30)$$

And:

$$Q_{out} = \sqrt{2\cdot g\cdot h_{SEM}}\cdot h_{SEM}\cdot l_{dam} \qquad m^3/s/cycle \qquad (31)$$

h_{SEM} — Head of added water on vehicle deck, based on principles of Static Equivalency Method (32)

Of note is use of single value of water head on the vehicle deck h_{SEM}. This value is derived with the Static Equivalent Method, well known from the previous stages of the project. h_{SEM} indicates the added head of water (i.e. water in addition to the static water inflow, see Figure 13) needed to be accumulated for the vessel to capsize after reaching "point-of-no-return" with heel angle near the GZ_{max}. It is assumed that the corresponding to h_{SEM} amount of floodwater reflects the measure of vessel resistance against the water ingress due to action of waves.

So, the remaining function is that of the probability density function of egress correction coefficient. On the bases of the hypothesis described above, this probability density function is found by comparing the egress rates estimated from Bernoulli equation for water head h_{SEM} at the deck edge for given amount of floodwater on the vehicle deck with flooding rates measured experimentally, see Figure 14.

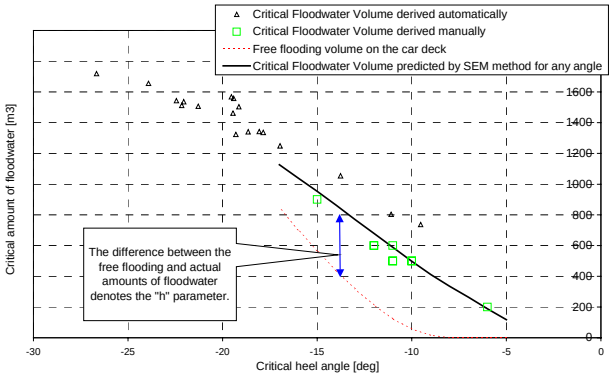

Figure 13 Correlation between critical heel angle and critical amount of floodwater on the car deck at the instant of capsize

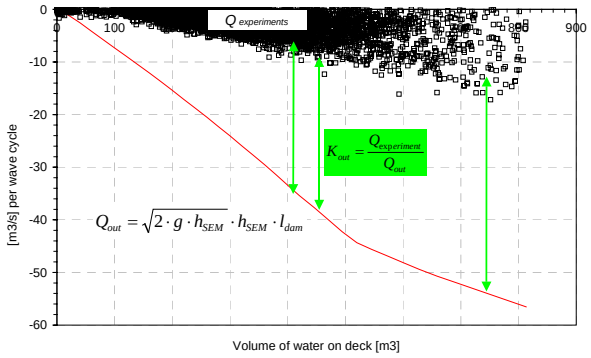

Figure 14 Floodwater egress rates based on Bernoulli equation with *h* corresponding to given amount of floodwater on the vehicle deck. The ratio of experimental rates to the numerical values (for h_{SEM}) is used to derive the spread of the egress coefficient K_{out} shown in (33)

As has been subsequently found out, the spread of the coefficient is independent on the amount of the water on deck, and can be approximated with the following function (33):

$$f_{K_{out}}(K) = 6.6 \cdot e^{-105 \cdot (K - 0.061)^2} \qquad (33)$$

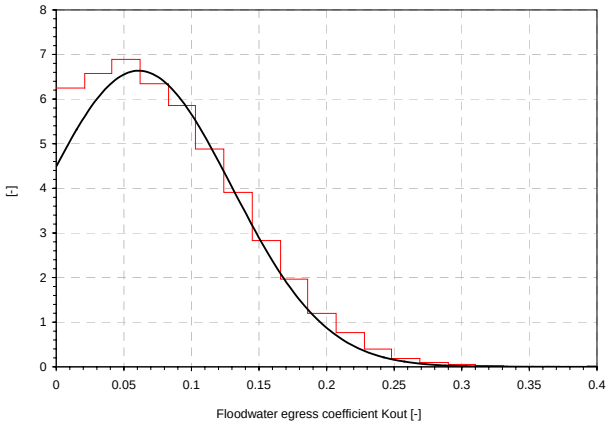

Figure 15 Fitted probability density function of egress coefficient, comparison with experimental data

4 Verification studies

The above technique might seem complicated, however most of the above integrand functions are standard in any computational package. The most complex of the whole procedure is actually deriving the h_{SEM} value, which has been facilitated by available and widely used today naval architecture packages for ship stability assessment, such as NAPA. Once the model is coded numerically, the actual information for assessment of ship survivability to be given as input is minimal.

In order to demonstrate practical application of the above method, an outline is given of the experimental data used, followed by a brief discussion of some details of the calculation, and finally followed by range of verification results obtained.

The model tests on survivability used were those performed at Denny Tank in Dumbarton, the model testing facility of the University of Strathclyde, in previous phase of this project as well as with the help from other projects. For the tests a 1:40 scale GRP model of Passenger Ro-Ro (PRR1) was used, see Table 1 and Figure 16 for the details. The model was equipped with 14 wave probes on the car deck and another two wave probes in front of the opening to measure the amount of floodwater on the car deck. Only the bilge keels were mounted as external appendages. The sea conditions were modelled according to JOHNSWAP wave energy spectrum, generated on the basis of linear theory of random processes. The parameters of the spectrum were determined according to the following relations:

$$\alpha = \frac{Hs}{\lambda},\ T_p = \sqrt{\frac{2 \cdot \pi \cdot \lambda}{g}},\ T_p = C \cdot \sqrt{Hs},\ C = \sqrt{\frac{2 \cdot \pi}{g \cdot \alpha}},$$

$$T_z = \frac{T_p}{1.49 - 0.102 \cdot \gamma + 0.0142 \cdot \gamma^2 - 0.00079 \cdot \gamma^3}$$

Where wave steepness α was chosen as 1/25 and 1/20. The spectral peakness parameter γ was chosen as 3.3. A range of sea states of H_s=1.0 – 6.25 [m], each of which was represented by at least 5 different time realisations, were pre-tested to ensure modelling of the environment with high accuracy ($\pm 1mm$ model scale in Hs). The model was removed from the tank and the wave measured by a fixed wave probe.

Table 1 Particulars of PRR1 vessel

Length between perpendiculars	170.00	m
Subdivision Length	178.75	m
Breadth	27.80	m
Depth to subdivision deck (G-Deck)	9.00	m
Depth to E-Deck	14.85	m
Draught	6.25	m
Displacement intact	17301.7	t
KMT	15.522	m
KG	12.892	m

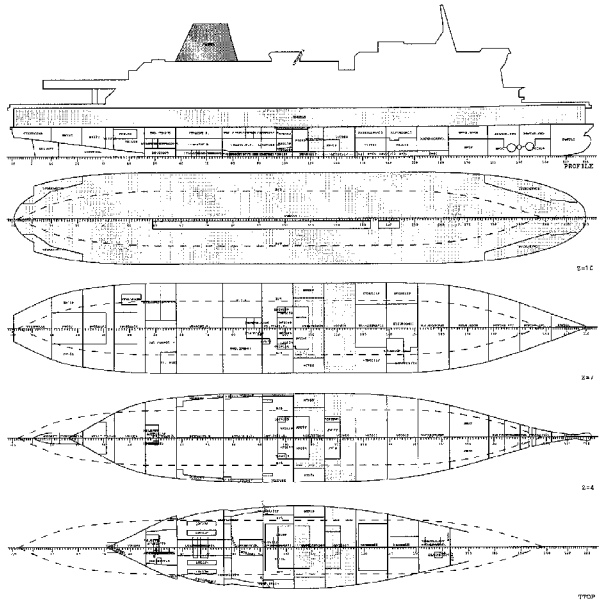

Figure 16 D901 damage case of PRR1

The model was placed in the tank, free to drift, beam-on to the waves and the survivability was tested for approximately five successive sea states, again, each one repeated at least five times, so that a clear distinction between capsize and survival cases could be derived. In total, 627 experiments were performed. The vessel conditions tested are given in Table 2, together with the reported survivability expressed in terms of H_s measured at the fixed probe with no model in the basin and the survivability predicted with the use of the above technique for assumed 320 cycles corresponding approximately to some 30 minutes.

As a way of illustrating the "mechanics" of the proposed method, two samples are chosen with illustration of the integrand functions of formulae (1).

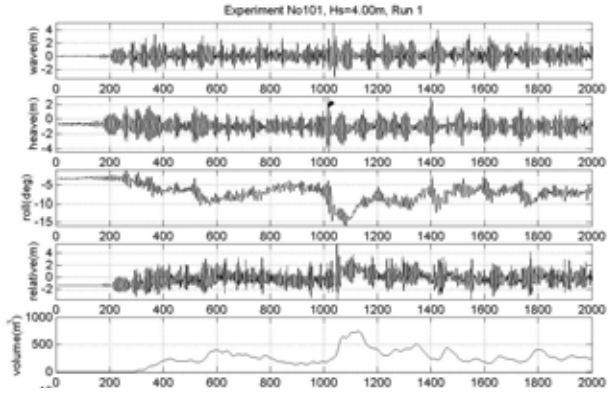

Figure 17 Time series for survivability tests of PRR1 vessel, "survive" case, H_s=4.0m.

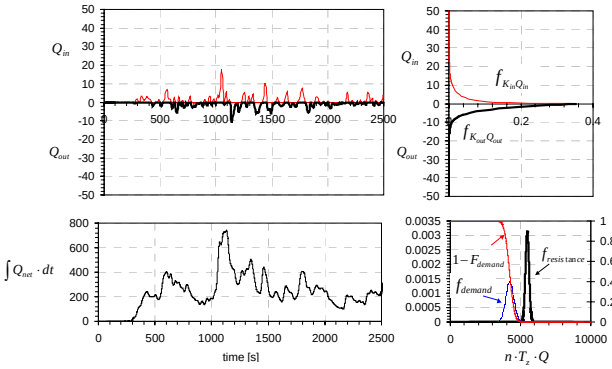

Figure 18 Assessment of survivability for PRR1 vessel, Run 101, 0% capsize case, n~320, Hs=4m, estimated failure probability p_f~0.

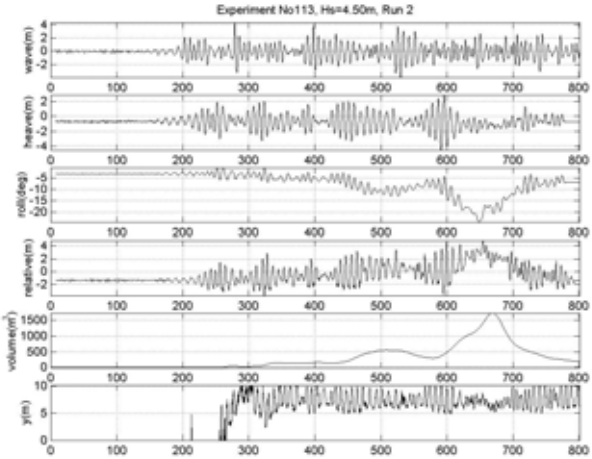

Figure 19 Time series for survivability tests of PRR1 vessel, "capsize" case, Hs=4.5m.

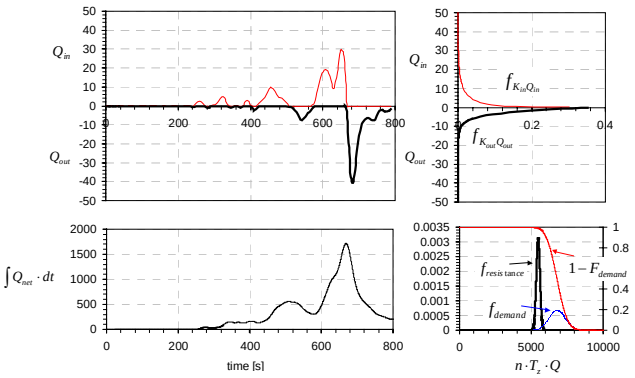

Figure 20 Assessment of survivability for PRR1 vessel, Run 113, 100% capsize case, n~320, Hs=4.5m, estimated failure probability p_f~1.

Table 2 Study cases

Case	Deck Height	Permeability	Initial Draught[m]	Initial Trim[deg]	KG[m]	Final Draught[m]	Final Trim[m]	Final Heel[deg]	Residual freeboard[m]	MBM	Experiment: Hs 0% Capsize	Experiment: Hs 100% Capsize	Pf: Hs 0% Capsize	Pf: Hs 100% Capsize
1	9	0.95	6.250	0.000	12.200	6.822	0.704	2.500	1.472	0.305	6.75		6	6.25
2	9	0.95	6.250	0.000	12.092	6.906	0.700	3.200	1.388	0.767	4	4.5	3.5	4.5
3	9	0.95	6.250	0.000	13.456	6.904	0.794	4.800	1.502	0.568	2.5	3.25	2.75	3.75
4	9	0.95	6.250	0.000	14.704	6.867	0.807	6.000	0.680	0.358	2	2	1.75	2.5
5	9	0.95	6.250	-1.000	12.200	6.942	-1.947	2.400	1.476	0.804	4	4.75	3.75	5
6	9	0.95	6.250	-1.000	12.092	6.937	-1.960	3.000	1.336	0.682	3	3.75	3.25	4.5
7	9	0.95	6.250	-1.000	13.456	6.927	-1.956	3.900	1.029	0.557	2.5	3	2.75	3.75
8	9	0.95	6.250	-1.000	14.704	6.893	-1.957	6.100	0.630	0.352			1.5	2
9	9	0.95	6.250	1.000	12.200	6.907	3.353	2.500	1.477	0.745	3.5	4.25	3.5	5
10	9	0.95	6.250	1.000	12.092	6.990	3.370	3.200	1.394	0.637			3.25	4.5
11	9	0.95	6.250	1.000	13.456	6.896	3.365	4.800	1.160	0.544			2.75	3.75
12	9	0.95	6.250	1.000	14.704	6.847	3.375	6.700	0.920	0.394			1.25	2
13	9	0.95	5.750	0.000	12.200	6.398	0.746	2.400	2.027	1.165			5	6.75
14	9	0.95	5.750	0.000	12.092	6.367	0.750	3.000	1.886	1.008	6.25		4.5	6
15	9	0.95	5.750	0.000	13.456	6.377	0.758	3.700	1.726	0.888	5	6.25	4	5.5
16	9	0.95	5.750	0.000	14.704	6.352	0.776	5.300	1.364	0.592	3.25	4.25	3.25	4.5
17	9	0.95	6.750	0.000	12.200	7.451	0.793	2.600	0.948	0.623	3	3.75	2.75	3.75
18	9	0.95	6.750	0.000	12.092	7.443	0.794	3.300	0.757	0.505	2	2.75	2.25	3
19	9	0.95	6.750	0.000	13.456	7.429	0.796	4.400	0.505	0.320	1.5	1.75	1.5	2.25
20	9	0.95	6.750	0.000	14.704									
21	9	0.95	6.250	-0.600	12.092	6.929	-0.842	3.000	1.339			4.5		
22	9	0.7	6.250	0.000	12.200	6.735	0.573	1.800	1.628	1.059			4.5	6
23	9	0.7	6.250	0.000	12.092	6.732	0.576	2.200	1.734	0.922	6.75	6.75	4.25	5.5
24	9	0.7	6.250	0.000	13.456	6.727	0.580	2.900	1.570	0.723	4	4.75	3.75	5
25	9	0.7	6.250	0.000	14.704	6.708	0.595	4.200	1.250	0.542	2.5	3	2	4
26	9	0.7	6.250	-1.000	12.200	6.748	-2.223	1.600	1.864	0.888	4.5	5.75	4.25	5.75
27	9	0.7	6.250	-1.000	12.092	6.745	-2.239	2.100	1.746	0.709	4	4.5	4	5.5
28	9	0.7	6.250	-1.000	13.456	6.741	-2.234	2.600	1.628	0.707			3.75	5
29	9	0.7	6.250	-1.000	14.704	6.728	-2.228	3.900	1.327	0.543			3	4.25

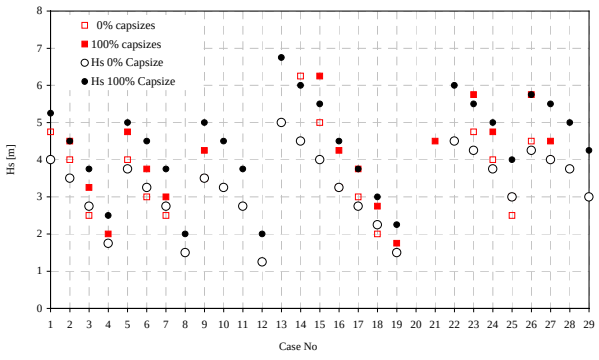

Figure 21 Survival boundaries for the test cases, comparison between experiment and the survival-time based technique

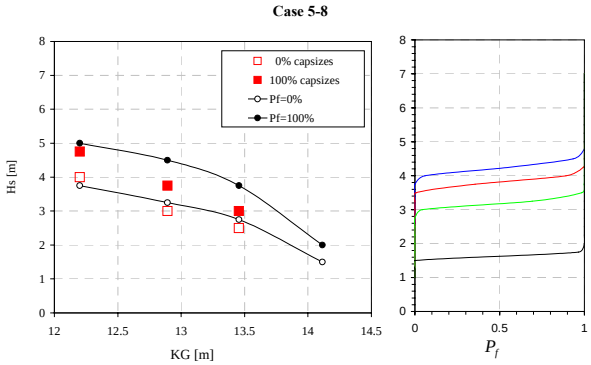

Figure 22 Survival boundaries for cases 5-8 and distribution of probability to capsize, comparison between experiment and the survival-time based technique

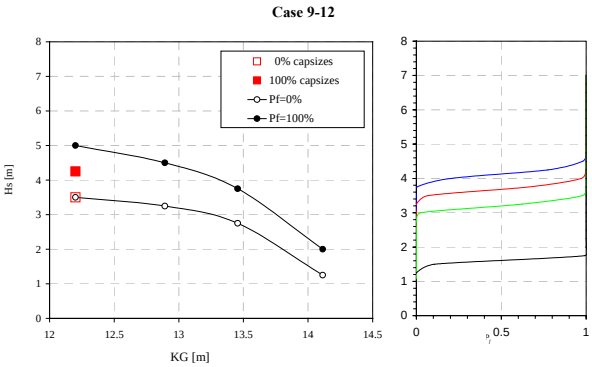

Figure 23 Survival boundaries for cases 9-12 and distribution of probability to capsize, comparison between experiment and the survival-time based technique

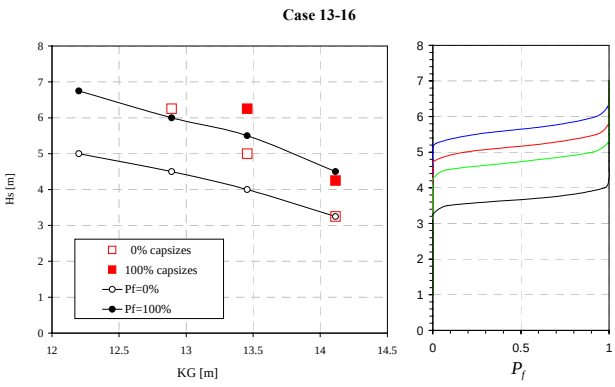

Figure 24 Survival boundaries for cases 13-16 and distribution of probability to capsize, comparison between experiment and the survival-time based technique

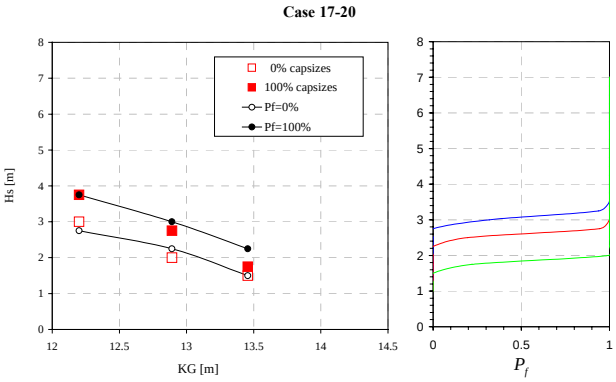

Figure 25 Survival boundaries for cases 17-20 and distribution of probability to capsize, comparison between experiment and the survival-time based technique

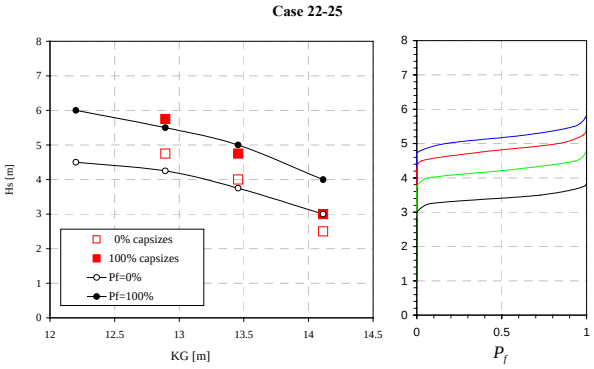

Figure 26 Survival boundaries for cases 22-25 and distribution of probability to capsize, comparison between experiment and the survival-time based technique

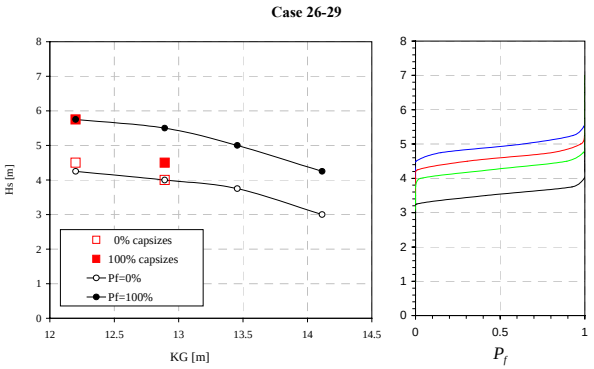

Figure 27 Survival boundaries for cases 26-29 and distribution of probability to capsize, comparison between experiment and the survival-time based technique